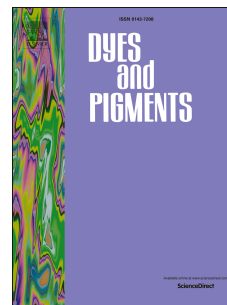


Accepted Manuscript

Development of near-infrared xanthene fluorescence probe for the highly selective and sensitive detection of cysteine

Yongquan Wu, Aiping Shi, Hong Zeng, Yuanyan Li, Huifang Li, Xiaoyong Chen, Wai-Yeung Wong, Xiaolin Fan



PII: S0143-7208(19)30528-5

DOI: <https://doi.org/10.1016/j.dyepig.2019.107563>

Article Number: 107563

Reference: DYPI 107563

To appear in: *Dyes and Pigments*

Received Date: 11 March 2019

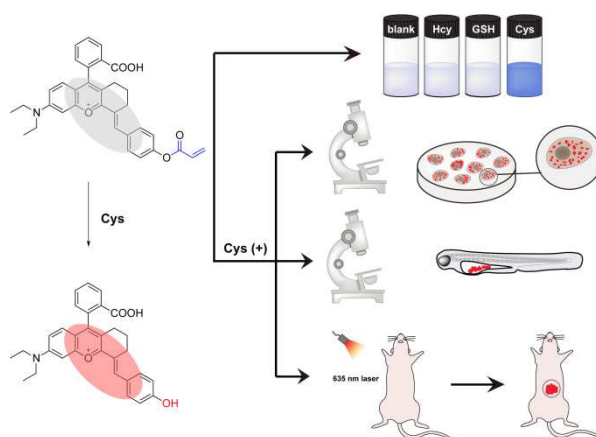
Revised Date: 13 May 2019

Accepted Date: 14 May 2019

Please cite this article as: Wu Y, Shi A, Zeng H, Li Y, Li H, Chen X, Wong W-Y, Fan X, Development of near-infrared xanthene fluorescence probe for the highly selective and sensitive detection of cysteine, *Dyes and Pigments* (2019), doi: <https://doi.org/10.1016/j.dyepig.2019.107563>.

This is a PDF file of an unedited manuscript that has been accepted for publication. As a service to our customers we are providing this early version of the manuscript. The manuscript will undergo copyediting, typesetting, and review of the resulting proof before it is published in its final form. Please note that during the production process errors may be discovered which could affect the content, and all legal disclaimers that apply to the journal pertain.

Graphical Abstract



A novel NIR xanthene fluorescence probe showed sensitive and selective response toward Cys, and was developed to detect endogenous Cys *in vivo*.

Development of Near-Infrared Xanthene Fluorescence Probe for the Highly Selective and Sensitive Detection of Cysteine

Yongquan Wu^{a,b}, Aiping Shi^a, Hong Zeng^a, Yuanyan Li^a, Huifang Li^a, Xiaoyong Chen^a,
Wai-Yeung Wong^{b*}, and Xiaolin Fan^{a*}

^a School of Chemistry and Chemical Engineering & Key Laboratory of Organo-Pharmaceutical Chemistry of Jiangxi Province, Gannan Normal University, Ganzhou 341000, P. R. China, E-mail: fanxl2013@gnnu.cn; Fax: +86 797 8393 536; Tel: +86 797 8393 670

^b Department of Applied Biology and Chemical Technology, The Hong Kong Polytechnic University, Hung Hom, Hong Kong, P. R. China, E-mail: wai-yeung.wong@polyu.edu.hk

Abstract: Abnormal levels of the biological thiol cysteine (Cys) have been shown to be associated with growth retardation, skin lesions, and neurotoxicity in humans. In order to fully elucidate the role of Cys in biological systems, its levels must be monitored through *in vitro* assays as well as in living cells and animals. Herein, we designed and synthesized a novel near-infrared xanthene fluorescence probe (NOF1) with an acrylate group as a trigger moiety to detect Cys over homocysteine and glutathione. The NOF1 probe exhibited a good selectivity and a high sensitivity toward Cys, with a detection limit of 210 nM. Additionally, NOF1 retained good sensitivity and selectivity in human plasma, with a good recovery of Cys within the range 98% to 102%. Importantly, the NOF1 probe was successfully applied to the fluorescence imaging of Cys in living cells, zebrafish, and mice, showing great potential for applications involving the detection of Cys both *in vitro* and *in vivo*.

Keywords: Cysteine, Xanthene fluorescence dye, Near-infrared, Fluorescence imaging

1 Introduction

Biological thiols such as cysteine (Cys), homocysteine (Hcy), and glutathione (GSH) play important roles in complex physiological systems[1,2], particularly in the maintenance of the appropriate redox status of proteins, cells, and organisms[3]. Cys

is an essential amino acid for metabolism and detoxification[4], and its abnormal levels in living systems have been associated with skin lesions, neurotoxicity, psoriasis, leucocyte loss, liver damage, and Parkinson's disease[5-9], among other illnesses. Therefore, the highly selective and sensitive detection of Cys is of great significance in biochemistry and biomedicine. Currently available Cys detection methods include capillary electrophoresis[10,11], high-performance liquid chromatography, and optical detectors[12-14]. However, these methods require complicated sample preparation procedures or pretreatment and cannot be used for the *in vivo* detection of Cys or in living cells. Nevertheless, in order to fully elucidate the role of Cys in biological systems, Cys levels must be monitored both *in vitro* and *in vivo* in living cells and animals[15,16]. Thus, the development of convenient and inexpensive methods for the real-time *in vivo* monitoring of Cys levels is required.

Fluorescence detection has been extensively studied due to its high sensitivity and selectivity, as well as its simplicity and facile application in biological sample assays[17-21]. To date, various fluorescent probes have been developed for the monitoring of Cys levels based on various mechanisms[3,22-27], and probes to detect Cys over Hcy and GSH have been reported[28,29]. However, numerous probes with emission and absorption wavelengths in the ultraviolet or visible region cannot be applied *in vivo* imaging due to their shallow penetration depth and animal background autofluorescence. Near-infrared (NIR) light (650–900 nm) has a lower energy, deeper tissue penetration, and reduced optical damage to biological samples compared to visible light, as well as minimum background interference from autofluorescence[30-33]. Therefore, the development of novel NIR emission probes for the rapid, highly selective, and sensitive detection of Cys both *in vitro* and *in vivo* is warranted.

Herein, we designed and synthesized a novel NIR emission xanthene fluorescence probe (NOF1) with acrylate groups acting as the trigger moiety probe that is able to sensitively and selectively detect Cys (Scheme 1). Furthermore, the NOF1 probe undergoes a rapid and selective response for Cys over Hcy and GSH with a lower

limit of detection (LOD) than the available techniques *in vitro*. Importantly, the NOF1 probe could be applied for the *in vivo* imaging of Cys in living cells, zebrafish, and mice due to its NIR emission, indicating a significant potential for biological applications.

2 Experimental sections

2.1 Materials and Methods

Materials. All commercial chemicals were purchased from commercial suppliers and used without further purification. All solvents were purified before use. 2-(4-diethylamino-2-hydroxybenzoyl) bezoic acid, cyclohexanone and HClO₄ (70%) were purchased from Shanghai Sain Chemical Technology Co., Ltd. Acryloyl chloride and potassium acetate were purchased from Adamas Regent Co., Ltd. 4-Hydroxybenzaldehyde was purchased from Aladdin Technology Co., Ltd. Et₃N was purchased from TCI (Shanghai) Chemical Industry Development Co., Ltd. Concentrated H₂SO₄ was purchased from Jiangsu Tong Sheng Chemical Reagent Co., Ltd. Anhydrous CH₂Cl₂ was purchased from J&K Scientific Ltd. MTT and PBS were purchased from Beyotime Biotechnology Co., Ltd (China). RPMI 1640 was purchased from Thermo Fisher Scientific Co., Ltd. N-ethylmaleimide (NEM) was also purchased from Adamas Regent Co., Ltd.

Methods. ¹HNMR (400 MHz) spectra was obtained on a BrukerDRX-400 spectrometer, with tetramethylsilane (TMS) as an internal standard (0 ppm) substances. The high resolution mass spectra (HRMS) spectra were measured with Fourier-transform ion cyclotron resonance mass spectrometry (FTICR-MS). UV-vis absorption spectra were recorded on a Shimadzu UV-2007 spectrophotometer. Fluorescence measurements were carried out on an Edinburgh FS5 fluorescence spectrometer. Fluorescence imaging of HeLa cells were obtained using Olympus FV1000 confocal fluorescence microscope (Japan Olympus Optical Co., Ltd). The absorbance value was measured using a Thermo Varioskan LUX micro-plate reader (ThermoFisher Scientific) in the MTT assay. *In vivo* fluorescence imaging was

performed with an *in vivo* imaging system (IVScpoe 7550, Shanghai CLINX Science Instruments Ltd., China).

2.2 Synthesis details

The synthesis routine of NOF1 and NOF1-Cys are shown at Scheme S1.

Synthesis of compound 1. Compound 1 was synthesized according to previous literature[34]. To a solution of 4-Hydroxybenzaldehyde (122 mg, 1 mmol) and Et₃N (1.4 mL, 10 mmol) in 15 mL of anhydrous CH₂Cl₂, acryloyl chloride (180 mg, 2 mmol) was added dropwise at 0 °C. After stirring at this temperature 90 min, the mixture was warmed to room temperature and stirred overnight. The solution was diluted with CH₂Cl₂ (30 mL), washed with H₂O (15 mL × 3) and dried over anhydrous Na₂SO₄. The solvent was removed in rotavapor. The crude product was purified by silica gel chromatography (PE/EA) to afford 59 mg (34%) of compound 1 as colorless oily liquid. ¹H NMR (400 MHz, CDCl₃) δ 10.00 (s, 1H), 7.98 – 7.90 (m, 2H), 7.37 – 7.31 (m, 2H), 6.65 (dd, J = 17.3, 1.1 Hz, 1H), 6.34 (dd, J = 17.3, 10.4 Hz, 1H), 6.08 (dd, J = 10.5, 1.1 Hz, 1H). ¹³C NMR (101 MHz, CDCl₃) δ 191.08 (s), 163.81 (s), 155.31 (s), 134.00 (s), 133.55 (s), 131.24 (s), 127.39 (s), 122.34 (s).

Synthesis of compound 2. Compound 2 was synthesized according to previous literature[35]. Cyclohexanone (3.3 mL, 32 mmol) was added dropwise to concentrated H₂SO₄ (50 mL) and cooled down to 0 °C. Then, 2-(4-diethylamino-2-hydroxybenzoyl) benzoic acid (5.01 g, 16 mmol) was added in portions with vigorous stirring. The reaction mixture was heated at 90 °C for 2 h, cooled down, and poured onto ice (200 g). Perchloric acid (70%; 3.5 mL) was then added, and the resulting precipitate was filtered off and washed with cold water (200 mL). Compound 2 obtained as a red solid was used for the next step without further purification. HRMS (ESI) C₂₄H₂₆NO₃⁺ [M+H]⁺: calcd, 377.1991; found, 377.2046.

Synthesis of NOF1. Into a 50 mL flask were added compound 3 (123 mg, 0.33 mmol), Compound 2 (59.9 mg, 0.35 mmol), potassium acetate (48 mg, 0.7 mmol) and acetic acid (5 mL). The mixture was heated to 90 °C for 12 h under nitrogen protection,

and the solvent was removed by the evaporation under the reduced pressure. The crude product was purified by silica gel chromatography ($\text{CH}_2\text{Cl}_2/\text{MeOH}=20:1$) to afford 20 mg (11%) of NOF1 as purple solid. ^1H NMR (400 MHz, CD_3OD) δ 8.01 (dd, $J = 6.8, 2.2$ Hz, 1H), 7.94 (s, 1H), 7.59 – 7.51 (m, 4H), 7.17 (d, $J = 8.6$ Hz, 2H), 7.08 (dd, $J = 6.4, 2.2$ Hz, 1H), 7.01 (s, 3H), 6.51 (d, $J = 17.4$ Hz, 1H), 6.30 (dd, $J = 17.3, 10.4$ Hz, 1H), 6.00 (d, $J = 9.7$ Hz, 1H), 3.59 – 3.53 (m, 4H), 2.86 (dt, $J = 10.6, 5.5$ Hz, 2H), 2.23 (dt, $J = 16.6, 5.8$ Hz, 2H), 1.72 (d, $J = 4.8$ Hz, 2H), 1.21 (t, $J = 7.1$ Hz, 6H). HRMS (ESI) $\text{C}_{34}\text{H}_{32}\text{NO}_5^+$ $[\text{M}+\text{H}]^+$: calcd, 534.2275; found, 534.2269.

Synthesis of NOF1-Cys. This material was prepared according to the reported literature[31]. 4-hydroxybenzaldehyde (0.10 g, 0.82 mmol) and compound 3 (0.34 g, 0.90 mmol) were reacted in 15 mL AcOH overnight, and then the work-up process was performed. NOF1-Cys was received as dark purple solid (0.10 g, 0.20 mmol), yield: 24%. ^1H NMR (400 MHz, MeOD) δ 8.13 (d, $J = 24.6$ Hz, 2H), 7.69 – 7.62 (m, 2H), 7.57 (d, $J = 8.3$ Hz, 2H), 7.17 (s, 4H), 6.92 (d, $J = 8.4$ Hz, 2H), 3.70 (q, $J = 7.1$ Hz, 4H), 2.98 (d, $J = 6.9$ Hz, 2H), 2.57 – 2.37 (m, 2H), 1.90 – 1.79 (m, 2H), 1.32 (t, $J = 7.0$ Hz, 6H). HRMS (ESI) $\text{C}_{31}\text{H}_{30}\text{NO}_4^+$ $[\text{M}]^+$: calcd, 480.2169; found, 480.2155.

2.3 UV-vis absorption and fluorescence spectra

Stock solutions of probe NOF1 (2 mM) was prepared in DMSO. Stock solutions of analyte (1–10 mM) were prepared in distilled water. The stock solutions of analyte were diluted to desired concentrations with distilled water when needed. For a typical optical measurements, probe NOF1 and NOF1-Cys were diluted to 10 μM in PBS (5 mM, pH=7.4) with 50% DMSO (v/v), respectively and 2 mL of the resulting solution was placed in a quartz cell. The amino acids titration of probe NOF1 spectrophotometric determination was carried out in PBS (5 mM, pH=7.4) with 50% DMSO (v/v). Various amino acids (20 μM) were titrated into a solution of probe NOF1 (10 μM), respectively. Before UV-vis absorption and photoluminescence spectra of the samples were measured, the solutions were kept at 37 $^\circ\text{C}$ for 10 min. For luminescence measurements, excitation was provided at 670 nm, and emission was collected from 685 to 850 nm. UV-visible spectra were recorded on

ShimadzuUV-2007 spectrometer and emission spectra were recorded on Edinburgh FS5 spectrometer.

Human plasma (1 mL) was deproteinized using acetonitrile (3 mL) and centrifuging at 8,000 rpm for 30 min. The supernatant was diluted in PBS buffer (pH =7.4, 5 mM). The Cys content in the plasma sample was determined using the same procedure above and the standard calibration curves.

2.4 Computational Details

These two compound NOF1 and NOF1-Cys were optimized at the density functional theory (DFT) level using the Becke's three-parameter hybrid exchange functional combined with the Lee-Yang-Parr correlation functional B3YLP[36] and the 6-31G(d,p) basis set[37]. Harmonic vibrational frequencies were calculated correspondingly at the same level to confirm each point corresponds to a minimum on the potential energy surface. Time-dependent DFT (TD-DFT) [38] calculations were performed to get the nature of the excited states based on the optimized structures. All calculations were performed with Gaussian 09 Rev. D. 01[39].

2.5 Cell culture and cytotoxicity of NOF1

The HeLa cell lines (human cervical epitheloid carcinoma) were provided by the Institute of Biochemistry and Cell Biology (Chinese Academy of Sciences). HeLa cells were grown in culture media (RPMI 1640) at 37 °C under a humidified atmosphere containing 5% CO₂ for 24 h. Cells were plated on 15 mm glass coverslips and allowed to adhere for 24 h.

The *in vitro* cytotoxicity was measured using a standard methyl thiazolyl tetrazolium (MTT) assay in HeLa cell lines. Cells growing in a 96-well flat-bottomed microplate (1×10^4 cells well⁻¹) in complete RPMI 1640 supplemented with 10% FBS (100 μ L well⁻¹) at 37 °C under 5% CO₂. After 24h, the sample (100 μ L well⁻¹) was added to the wells of the test group at concentrations of 5, 10, 15, 20, 25, 30 μ M, respectively. Added RPMI 1640 supplemented with 0.2 % DMSO (100 μ L well⁻¹) to control group. The cells incubated for 24 h. Thereafter, combined 20 μ L MTT/PBS

solutions (5 mg mL^{-1}) were added to every well and keep incubating at $37 \text{ }^{\circ}\text{C}$ under 5% CO_2 . After 5 h remove solution and added DMSO ($150 \text{ } \mu\text{L well}^{-1}$) to wells. The quantity of the formazan product formed as measured the amount of OD 490 (absorbance value) of each well referenced at 690 nm (OD 690) is directly proportional to the number of living cells in the culture. Each experiment was done in quadruplicate. The relative viability (%) of cell growth related to control wells containing cell culture medium without NOF1 was calculated by $[\text{OD}]_{\text{expt}}/[\text{OD}]_{\text{control}} \times 100$, where $[\text{OD}]_{\text{expt}}$ is the absorbance of the test sample and $[\text{OD}]_{\text{control}}$ is the absorbance of control sample.

2.6 Confocal imaging for living cells

The cells were incubated for 24 h prior to the imaging experiments. The living cells were stained with $10 \text{ } \mu\text{M}$ probe NOF1 for 30 min at $37 \text{ }^{\circ}\text{C}$ under 5% CO_2 . For control experiments, the cells were pretreated with thiol trapping reagent, N-ethylmaleimide (NEM, $100 \text{ } \mu\text{M}$) for 30 min at $37 \text{ }^{\circ}\text{C}$, followed by washing with PBS buffer ($2 \text{ mL} \times 3$ times), and incubated with probe NOF1 ($10 \text{ } \mu\text{M}$) for 30 min at $37 \text{ }^{\circ}\text{C}$ under 5% CO_2 . Moreover, HeLa cells were pretreated with Cys ($100 \text{ } \mu\text{M}$) for 120 min and then further incubated with NOF1 ($10 \text{ } \mu\text{M}$) for 30 min at $37 \text{ }^{\circ}\text{C}$ under 5%. The cells were imaged under an Olympus FV1000 confocal luminescence microscope. For NOF1, excited at 635 nm, emission was collected by a range 670–770 nm equipped with a 40 \times -oil immersion objective lens.

2.7 Visualizing Cys in the living zebrafish

4-day old zebrafishes were grew in E3 embryo media (15 mM NaCl , 0.5 mM KCl , 1 mM MgSO_4 , 1 mM CaCl_2 , $0.15 \text{ mM KH}_2\text{PO}_4$, $0.05 \text{ mM Na}_2\text{HPO}_4$, 0.7 mM NaHCO_3 , pH 7.5). As the control group, the 4-day-old zebrafish was incubated with probe NOF1 ($10 \text{ } \mu\text{M}$) for 30 min in E3 media at $28 \text{ }^{\circ}\text{C}$. Other group, the 4-day-old zebrafish was pre-incubated with $200 \text{ } \mu\text{M}$ NEM for 30 min and then incubated with $10 \text{ } \mu\text{M}$ NOF1 for 30 min. After washing with E3 media to remove the remaining NEM, the zebrafish was further incubated with $10 \text{ } \mu\text{M}$ of probe NOF1 in E3 media for 30 min at $28 \text{ }^{\circ}\text{C}$. After washing with E3 media, the zebrafish was imaged by

fluorescence microscopy. The zebrafishes were anesthetized by Tricain, and the low melting point Agarose served as fixing reagent during imaging.

2.8 Fluorescence imaging *in vivo*

Animal procedures were in agreement with the guidelines of the Institutional Animal Care and Use Committee of Gannan Normal University and performed in accordance with the institutional guidelines for animal handling. *In vivo* fluorescence imaging was performed with a modified luminescence *in vivo* imaging system (IVScpoe 7550, Shanghai CLINX Science Instruments Ltd., China). In this system, two external 0–5 W adjustable CW 635nm lasers (Changchun Laser Optoelectronics Technology Ltd., China) and an Andor CCD (IKON-M934BV, Andor Technology Ltd., UK) were used as the excitation sources and the signal collector, respectively. Firstly, the mice was anaesthetized in advance with 100 μ L chloral hydrate (4% wt. aqueous solution) and placed carefully into living animal imaging system. Furthermore, the mouse was subcutaneous injected with 50 μ L of 25 μ M probe NOF1 in saline. NIR fluorescence images of the living mice were performed at different time. In addition, *in vivo* fluorescence imaging system, emission at 680–780 nm was collected with a pass filter (Semrock, INC) under excitation at 635 nm. Images of fluorescence signal were analyzed with Kodak Molecular Imaging Software.

3 Results and Discussion

3.1 Design and synthesis

The NOF1 probe was constructed using a xanthene derivative as the NIR fluorophore and an acrylate moiety as the reaction site. Xanthene derivatives possess a large molar extinction coefficient, a high fluorescence quantum yield, and good light stability, among other properties[40,41]. Furthermore, the acrylate moiety has been shown to act as an efficient reaction site for biothiols through an addition-cyclization reaction mechanism[42,43], which generally leads to faster reaction kinetics with Cys than with Hcy or GSH[44-46]. The addition-cyclization reaction leads to the formation of a NOF1-Cys product with innate fluorescence. Masking of the phenolic OH with an acrylate group, an efficient electron acceptor, quenches NOF1-Cys

fluorescence, yet Cys fluorescence is selectively recovered by the removal of the masking group through addition-cyclization conjugation (Scheme 2). The NOF1 probe was synthesized through the reaction of intermediate compounds 1 and 2 (Scheme S1). Furthermore, the chemical structure of NOF1 was confirmed by ^1H -nuclear magnetic resonance (NMR) and high-resolution mass spectroscopy (HR-MS). The detailed synthetic procedures and structure characterization methods were provided in the Experimental Section and Supporting Information (see Figures S8-S14).

3.2 UV-vis absorption and fluorescence spectra

The absorption and emission spectra of compounds NOF1 and NOF1-Cys are shown in Figure S1. As expected, the NOF1 probe showed a weak fluorescence due to fluorophore quenching by the carbon-carbon double bond [34]. However, NOF1-Cys showed significant NIR fluorescence with a maximum absorption at 670 nm and an emission peak at 741 nm.

UV-vis absorption and fluorescence spectral changes of NOF1 (10 μM) reacting with different Cys concentrations (from 0 to 1.4 eq.) in PBS (5 mM, pH =7.4) with 50% DMSO (v/v) at 37 $^\circ\text{C}$ for 10 min (Figure S3) were investigated. The 10 μM NOF1 probe solution showed a major absorption peak at approximately 550 nm (Figure 1a). Upon Cys addition, the intensity of the 550 nm absorption band decreased along with an increase in the intensity of a new band at approximately 670 nm, leading to a 120 nm red shift. The growth in absorption intensity at 670 nm was attributed to deacylation via the response of the NOF1 probe to Cys. Simultaneously, the solution color changed from purple to blue. Thus, this phenomenon suggests that it is feasible for Cys to be detected by the “naked-eye”. Furthermore, the absorption intensities of the NOF1 probe with different Cys concentrations showed a linear correlation in the range of 0–0.8 equivalents of Cys (Figure S2).

Fluorescence titration experiments of the NOF1 probe with Cys showed a gradual increase in fluorescence intensity upon Cys addition (from 0 to 1.4 eq.) to the NOF1 solution (Figure 1b), with maximum value reaching at 741 nm under excitation at 670

nm (Figure S3). The intensity of the emission peak at 741 nm was gradually enhanced by the removal of the masking group through the addition-cyclization conjugation to the acrylate moiety (Scheme 1). The plot of fluorescence intensities at 741 nm against Cys concentration in the range 2–10 μM (0.2–1.0 eq.) showed a linear fit ($R^2 = 0.992$) (Figure S4), with a Cys LOD as low as 0.21 μM . The LOD was calculated using the formula $\text{LOD} = 3r/S$, where r is the standard deviation of blank measurements and S is the slope of the calibration curve. These results indicate the possibility of quantitative Cys detection within a good linear range. Furthermore, the excitation and emission of the NOF1 probe are both within the NIR range, thus allowing adequate sensitivity for the detection of Cys in biological systems.

3.3 Selectivity of NOF1 for Cys

A successful biological probe must have a suitably high selectivity. Therefore, we first confirmed the specific selectivity of the NOF1 probe to Cys as well as to other thiols with similar structures (Hcy and GSH). The time-dependent fluorescence response spectra were then determined by monitoring the fluorescence intensity changes in the reaction mixture. At 670 nm excitation, the NOF1 probe was almost non-emissive and stable for 0–10 min (Figure 2a). In contrast, following the addition of 2.0 eq. of Cys, the emission intensity at 741 nm showed an initial rapid increase, reaching a maximum within 10 min, suggesting a complete sensing response. Similar experiments using Hcy and GSH exhibited a minor increase in fluorescence, and required a longer time to reach the maximum intensity. Furthermore, the color change in the NOF1 solution in the presence of Cys, Hcy, and GSH could be optically observed (Figure 2a, inset). Moreover, changes in emission spectra were also examined, showing a similar trend (Figure 2b). Thus, the NOF1 probe can be used to effectively distinguish Cys from Hcy and GSH.

The observed differences between Cys and both Hcy and GSH can be attributed to the kinetic rate of the intramolecular adduct-cyclization reactions. The intramolecular cyclization reaction with Cys leads to the formation of a seven-membered ring [4,47, 48], whereas that with Hcy leads to the formation of an eight-membered ring;

therefore, the former is kinetically more favorable. In contrast, the intramolecular cyclization reaction with GSH is sterically hindered by the bulkiness of its tripeptide, leading to the formation of a conjugated thio-ether.

To further assess the selectivity of NOF1 toward Cys, the sensory responses to the amino acids alanine (Ala), arginine (Arg), asparagine (Asn), aspartic acid (Asp), glutamic acid (Glu), glutamine (Gln), histidine (His), isoleucine (Ile), leucine (Leu), lysine (Lys), phenylalanine (Phe), proline (Pro), serine (Ser), threonine (Thr), and tyrosine (Tyr) were also investigated. The absorption spectra changes of NOF1 after incubation with 10.0 eq. of the corresponding amino acid and Cys for 10 min at 37 °C showed that only Cys exhibited an obvious red-shift of maximum absorbance from 552 to 670 nm (Figure 3a), corresponding to the color change from purple to blue (Figure 3b). In addition, fluorescence spectra showed that only Cys exhibited a marked off-on response with enhanced fluorescence at 741 nm when excited by 670 nm light; the remaining amino acids revealed only a slight fluorescence enhancement (Figure S5). Thus, the NOF1 probe has a good selectivity toward Cys and could be used for its specific detection.

The above results showed that the NOF1 probe undergoes NIR emission, enhanced fluorescence, and is highly sensitive and selective toward Cys. Therefore, its application in bio-samples was examined. Therefore, its application in bio-samples was examined.

3.4 Reaction mechanism

To verify the sensing mechanism proposed in Scheme S2, the UV-Vis and fluorescence spectra of NOF1 (10 μ M), NOF1+Cys (10 μ M NOF1 reacting with 2.0 eq. Cys), and NOF1-Cys (10 μ M) were obtained. The final UV-Vis and fluorescence spectra were the same for both the mixture of NOF1 reacting with Cys (2.0 eq.) and for NOF1-Cys, demonstrating that the reaction product from NOF1+Cys was NOF1-Cys. Thus, the transformation process from NOF1 to NOF1-Cys was confirmed by the spectra change (Figure 4). HR-MS analysis of NOF1 and the product of NOF1+Cys further confirmed the above mechanism (Figure 5). NOF1

showed a characteristic peak of m/z 534.2269 ($[M+H]^+$ calculated value 534.2275). Additionally, the NOF1+Cys product exhibited a characteristic peak of m/z 480.2185 ($[M+H]^+$ calculated value m/z 480.2169). Based on these results and previous reports, we confirm that the reaction mechanism between NOF1 and Cys follows that indicated in Scheme 2. Namely, the NOF1 probe reacts with Cys through a conjugation addition and is followed by intramolecular cyclization to produce NOF1-Cys accompanied by a release of fluorescence. To better understand the photophysical properties of the NOF1 and NOF1-Cys, theoretical calculations were also performed through the time-dependent density functional theory (TD-DFT) (Figure S6). The energies for the frontier MOs as well as their corresponding HOMO-LUMO gaps are listed in Table S1. For NOF1-Cys, the π electrons on the HOMO were essentially distributed in the xanthene backbone and Ar-OH group. In contrast, the π electrons on the HOMO were mostly distributed in the xanthene backbone and little on the Ar-O group of NOF1. The π electrons on the LUMO primarily resided on the xanthene backbone both for NOF1 and NOF1-Cys. Herein, the excitation from the LUMO to HOMO transition thus induced the strong fluorescence observed for NOF1-Cys. The above results therefore successfully demonstrate that the sensing mechanism of the NOF1 probe is responsive to Cys and formed the NOF1-Cys.

3.5 Application of NOF1 in the detection of Cys in human plasma

Despite the existence of fluorescent probes able to detect Cys, these have rarely been applied in the determination of Cys in human plasma. Herein, the NOF1 probe has been used to assess Cys in human plasma samples appropriately diluted to fit the linear detection requirements. The average concentration of Cys in human plasma was shown to be approximately 166.4 μM (Table 1), which is in agreement with the reported results (130 to 290 μM Cys in human plasmas)[49,50]. Furthermore, Cys was added to the plasma in different concentrations to determine the recovery using the proposed method. The Cys recoveries ranged from 98% to 102% (Table 1), with a

relative error of no more than 5%, suggesting that the proposed method has great potential for the determination of Cys in real samples.

3.6 Cell cytotoxic assays and cell imaging

In order to pursue its application *in vivo*, its cytotoxicity was assessed. HeLa cells were treated with different concentrations of NOF1 (up to 30 μM) and the toxicity was assessed (Figure S7). At a 10 μM NOF1 concentration, cell viability remained unchanged after 24 h incubation, with more than 95% of cells remaining viable. When the NOF1 concentration was increased to 30 μM , cell viability remained above 80%. Furthermore, no sub-cellular apoptotic changes or significant cell death were observed following incubation with working concentrations required for imaging (5 μM for cell imaging and 10 μM for *in vivo* imaging), with cell viability remaining above 90%. In general, the NOF1 probe exhibited a low cytotoxicity when used within the concentrations and incubation periods required for imaging.

In order to prove that the NOF1 probe has a practical utility for intracellular Cys detection in living cells, confocal luminescence imaging was performed. When HeLa cells were incubated with NOF1 (5 μM) for 30 min, an obvious intracellular NIR fluorescence was observed (Figure 6a). However, when HeLa cells were pretreated with N-ethylmaleimide (a known thiol trapping reagent) for 120 min, followed by incubation with NOF1 (5 μM) for 30 min, the cells showed a weaker fluorescence (Figure 6b). In addition, following HeLa cells pretreatment with Cys (100 μM) for 120 min, followed by incubation with NOF1 (5 μM) for 30 min at 37 °C, a marked enhancement of NIR fluorescence was observed (Figure 6c). These results indicate that the probe NOF1 possesses good membrane permeability and is able to detect changes in intracellular Cys in living cells, holding great potential for biological applications.

3.7 Visualizing Cys in living zebrafish

We further investigated the ability of the NOF1 probe to visualize Cys in living zebrafish. The 4-day-old zebrafish incubated with 5 μM NOF1 for 30 min displayed

significant fluorescence (Figure 7a). Interestingly, the fluorescence in the zebrafish was not uniformly distributed, with the zebrafish yolk sac showing much stronger fluorescence. It is likely that the NOF1 probe was uniformly distributed in zebrafish, whereas Cys was not[51]; nevertheless, current evidence does not allow us to completely exclude the non-uniform distribution of the probe in zebrafish. Conversely, 4-day-old zebrafish pre-incubated with 200 μM N-ethylmaleimide showed minimal fluorescence (Figure 7b), demonstrating that the NOF1 probe is tissue-permeable and that the fluorescence generation results from the NOF1 probe interacting with Cys in the living zebrafish.

3.8 Fluorescence imaging *in vivo*

On the basis of the probe's NIR optical property, the NOF1 probe was explored as a tool for imaging of Cys in the living mouse. *In vivo* imaging of Cys using NOF1 was performed in living BALB/c nude mice. Firstly, the living mice were subcutaneous injected with 50 μL of 25 μM NOF1. As shown in Figure 8a, weak emission signals of mice were detected 5 min after the injection of NOF1, and then the fluorescence was enhanced after 30 min (Figure 8b). This was induced by the interaction between NOF1 probe and endogenous Cys. Therefore, the above results demonstrate that the NOF1 probe possesses the ability to sense Cys in living animals.

Conclusion

In conclusion, a novel NIR xanthene fluorescent NOF1 probe for the highly selective and sensitive detection of Cys over Hcy, GSH, and other amino acids was synthesized. The addition-cyclization conjugation reaction of Cys toward the acrylate moiety in the NOF1 probe results in the cleavage of the acrylate moiety and release of a free phenolic OH, thereby inducing a significant enhancement of fluorescence. This was confirmed by spectral changes and HR-MS. Importantly, the NOF1 probe exhibited a high selectivity and sensitivity towards Cys with a low LOD of 210 nM *in vitro*, as well as allowing the imaging of Cys in living cells, zebrafish, and *in vivo*. Therefore, this novel probe has great potential for applications involving the detection

of Cys both *in vitro* and *in vivo*. The present results offer valuable information and create a new platform for the design of NIR-emitting probes based on xanthene derivatives for fluorescence detection and imaging *in vivo*.

Acknowledgments

This work was supported by Natural Science Foundation of China (No. 21501031 and 51478123), and Hong Kong Polytechnic University (1-ZE1C and 1-YW2T). Wu et al. gratefully acknowledges Dr. Huiqiang Lu of Jinggangshan University for experimental support in zebrafish imaging.

References

- [1] Weerapana E, Wang C, Simon GM, Richter F, Khare S, Dillon MB. Quantitative reactivity profiling predicts functional cysteines in proteomes. *Nature* 2010;468:90–5.
- [2] Isokawa M, Shimosawa T, Funatsu T, Tsunoda M. Determination and characterization of total thiols in mouse serum samples using hydrophilic interaction liquid chromatography with fluorescence detection and mass spectrometry. *J Chromatogr B Analyst Technol Biomed Life Sci* 2016;101:959–65.
- [3] Fu Z H, Han X, Shao Y, Fang J, Zhang ZH, Wang YW. Fluorescein-Based Chromogenic and Ratiometric Fluorescence Probe for Highly Selective Detection of Cysteine and Its Application in Bioimaging. *Anal Chem* 2017;89:1937–44.
- [4] Yang X, Guo Y, Strongin RM. Conjugate addition/cyclization sequence enables selective and simultaneous fluorescence detection of cysteine and homocysteine. *Angew Chem Int Ed* 2011;50:10690–3.
- [5] Shahrokhian S. Lead Phthalocyanine as a Selective Carrier for Preparation of a Cysteine-Selective Electrode. *Anal Chem* 2001;73:5972–8.
- [6] Townsend DM, Tew KD, Tapiero H. The importance of glutathione in human disease. *Biomed Pharmacother* 2003;57:145–55.

- [7] Gazit V, Ben-Abraham R, Coleman R. A. Weizman, Y. Katz, Cysteine-induced hypoglycemic brain damage: an alternative mechanism to excitotoxicity. *Amino Acids* 2004;26: 63–8.
- [8] Li Q, Guo Y, Shao S. A BODIPY based fluorescent chemosensor for Cu(II) ions and homocysteine/cysteine. *Sens Actuators B: Chem* 2012;171: 872–7.
- [9] Dai X, Wu QH, Wang PC, Tian J, Xu Y, Wang SQ. A simple and effective coumarin-based fluorescent probe for cysteine. *Biosens Bioelectron* 2014;59: 35–9.
- [10] Zhou M, Ding J, Guo L-p, Shang Q-k. Electrochemical Behavior of l-Cysteine and Its Detection at Ordered Mesoporous Carbon-Modified Glassy Carbon Electrode. *Anal Chem* 2007;79: 5328–35.
- [11] de Carvalho Castro e Silva C, Breikreitz MC, Santhiago M, Corrêa CC, Kubota LT. Construction of a new functional platform by grafting poly(4-vinylpyridine) in multi-walled carbon nanotubes for complexing copper ions aiming the amperometric detection of l-cysteine. *Electrochim Acta* 2012;71: 150-8.
- [12] Jin W, Wang Y. Determination of cysteine by capillary zone electrophoresis with end-column amperometric detection at a gold/mercury amalgam microelectrode without deoxygenation. *J Chromatogr A* 1997;769:307–14.
- [13] Chwatko G, Bald E. Determination of cysteine in human plasma by high-performance liquid chromatography and ultraviolet detection after pre-column derivatization with 2-chloro-1-methylpyridinium iodide. *Talanta* 2000;52:509–15.
- [14] Ivanov AR, Nazimov IV, Baratova L, Lobazov AP, Popkovich GB. Determination of biologically active low-molecular-mass thiols in human blood: III. Highly sensitive narrow-bore isocratic reversed-phase high-performance liquid chromatography with fluorescence detection. *J Chromatogr A* 2001;913:315–8.
- [15] Peng T, Wong NK, Chen XM, Chan YK, Ho DHH, Sun ZN. Molecular Imaging of Peroxynitrite with HKGreen-4 in Live Cells and Tissues. *J Am Chem Soc* 2014;136:11728–34.
- [16] Xu J, Pan J, Jiang X, Qin C, Zeng L, Zhang H. A mitochondria-targeted ratiometric fluorescent probe for rapid, sensitive and specific detection of biological SO₂ derivatives in living cells. *Biosens Bioelectron* 2016; 77:725–32.

- [17] Chen X, Pradhan T, Wang F, Kim JS, Yoon J. Fluorescent chemosensors based on spiroring-opening of xanthenes and related derivatives. *Chem Rev* 2012; 112:1910–56.
- [18] Yang Y, Zhao Q, Feng W, Li F. Luminescent chemodosimeters for bioimaging. *Chem Rev* 2013;113: 92–270.
- [19] Teng Y, Jia X, Li J, Wang E. Ratiometric Fluorescence Detection of Tyrosinase Activity and Dopamine Using Thiolate-Protected Gold Nanoclusters. *Anal Chem* 2015;87:4897–902.
- [20] Zhang H, Liu J, Sun Y-Q, Huo Y, Li Y, Liu W. A mitochondria-targetable fluorescent probe for peroxynitrite: fast response and high selectivity. *Chem Commun* 2015;51:2721–4.
- [21] Fan WL, Huang XM, Shi XM, Wang Z, Lu ZL, Fan CH. A simple fluorescent probe for sensing cysteine over homocysteine and glutathione based on PET. *Spectrosc Acta Pt A-Molec Biomolec Spectr* 2017;173:918–23.
- [22] Rusin O, Luce NN St, Agbaria RA, Escobedo JO, Jiang S, Warner IM. Visual Detection of Cysteine and Homocysteine. *J Am Chem Soc* 2004;126:438–9.
- [23] Tang B, Xing Y, Li P, Zhang N, Yu F, Yang G. A Rhodamine-Based Fluorescent Probe Containing a Se–N Bond for Detecting Thiols and Its Application in Living Cells. *J Am Chem Soc* 2007;129:11666–7.
- [24] Zhang M, Yu M, Li F, Zhu M, Li M, Gao Y. A Highly Selective Fluorescence Turn-on Sensor for Cysteine/Homocysteine and Its Application in Bioimaging. *J Am Chem Soc* 2007;129:10322–3.
- [25] Yi L, Li H, Sun L, Liu L, Zhang C, Xi Z. A highly sensitive fluorescence probe for fast thiol-quantification assay of glutathione reductase. *Angew Chem Int Ed* 2009;48:4034–7.
- [26] Jia MY, Niu LY, Zhang Y, Yang QZ, Tung CH, Guan YF. BODIPY-based fluorometric sensor for the simultaneous determination of Cys, Hcy, and GSH in human serum. *ACS Appl Mater Inter* 2015;7:5907–14.

- [27] Cao X, Wu Y, Liu K, Yu X, Wu B, Wu H, Gong Z, Yi T. Iridium complex triggered white-light-emitting gel and its response to cysteine. *J Mater Chem* 2012; 22: 2650–7.
- [28] Yin K, Yu F, Zhang W, Chen L. A near-infrared ratiometric fluorescent probe for cysteine detection over glutathione indicating mitochondrial oxidative stress in vivo. *Biosens Bioelectron* 2015;74:156–64.
- [29] Zhang J, Wang J, Liu J, Ning L, Zhu X, Yu B. Near-Infrared and Naked-Eye Fluorescence Probe for Direct and Highly Selective Detection of Cysteine and Its Application in Living Cells. *Anal Chem* 2015;87: 4856–63.
- [30] Wrobel AT, Johnstone TC, Deliz Liang A, Lippard SJ, Rivera-Fuentes P. A fast and selective near-infrared fluorescent sensor for multicolor imaging of biological nitroxyl (HNO). *J Am Chem Soc* 2014;136:4697–705.
- [31] Liu K, Shang H, Kong X, Ren M, Wang JY, Liu Y. A novel near-infrared fluorescent probe for H₂O₂ in alkaline environment and the application for H₂O₂ imaging in vitro and in vivo. *Biomaterials* 2016;100:162–71.
- [32] Fang Y, Chen W, Shi W, Li H, Xian M, Ma H. A near-infrared fluorescence off-on probe for sensitive imaging of hydrogen polysulfides in living cells and mice in vivo. *Chem Commun* 2017;53:8759–62.
- [33] Guo J, Yang S, Guo C, Zeng Q, Qing Z, Cao Z. Molecular Engineering of alpha-Substituted Acrylate Ester Template for Efficient Fluorescence Probe of Hydrogen Polysulfides. *Anal Chem* 2018;90:881–7.
- [34] Han C, Yang H, Chen M, Su Q, Feng W, Li F. Mitochondria-Targeted Near-Infrared Fluorescent Off-On Probe for Selective Detection of Cysteine in Living Cells and in Vivo. *ACS Appl Mater Inter* 2015;7:27968–75.
- [35] Yuan L, Lin W, Yang Y, Chen H. A unique class of near-infrared functional fluorescent dyes with carboxylic-acid-modulated fluorescence ON/OFF switching: rational design, synthesis, optical properties, theoretical calculations, and applications for fluorescence imaging in living animals. *J Am Chem Soc* 2012;134:1200–11.
- [36] Becke AD, Density-functional thermochemistry. III. The role of exact exchange. *J Chem Phys* 1993; 98: 5648–52.

- [37] Krishnan R, Binkley JS, Seeger R, Pople JA. Self-consistent molecular orbital methods. XX. A basis set for correlated wave functions. *J Chem Phys* 1980;72:650–4.
- [38] Fantacci S, De Angelis F, Selloni A. Absorption Spectrum and Solvatochromism of the [Ru(4,4'-COOH-2,2'-bpy)₂(NCS)₂] Molecular Dye by Time Dependent Density Functional Theory. *J Am Chem Soc* 2003;125:4381–7.
- [39] Frisch MJ, Trucks GW, Schlegel HB, Scuseria GE, Robb MA, Cheeseman J R. Gaussian 09, Revision D. 01; Gaussian, Inc., Wallingford CT, 2013.
- [40] Kumar R, Shin WS, Sunwoo K, Kim WY, Koo S, Bhuniya S. Small conjugate-based theranostic agents: an encouraging approach for cancer therapy. *Chem Soc Rev* 2015;44:6670–83.
- [41] Dong B, Song X, Kong X, Wang C, Zhang N, Lin W. Two-photon red-emissive fluorescent probe for imaging nitroxyl (HNO) in living cells and tissues. *J Mater Chem B* 2017;5:5218–24.
- [42] Zhou X, Guo D, Jiang Y, Gong D-M, Zhao X-J, Zhou L-Y. A novel AIEE and EISPT fluorescent probe for selective detection of cysteine. *Tetrahedron Lett* 2017;58:3214–8.
- [43] Zhu B, Guo B, Zhao Y, Zhang B, Du B. A highly sensitive ratiometric fluorescent probe with a large emission shift for imaging endogenous cysteine in living cells. *Biosens Bioelectron* 2014;55:72–5.
- [44] Matsumoto T, Urano Y, Shoda T, Kojima H, Nagano T. A thiol-reactive fluorescence probe based on donor-excited photoinduced electron transfer: Key role of ortho substitution. *Org Lett* 2007;9:3375–7.
- [45] Liu XJ, Yang DL, Chen WQ, Yang L, Qi FP, Song XZ. A red-emitting fluorescent probe for specific detection of cysteine over homocysteine and glutathione with a large Stokes shift. *Sens Actuators B: Chem* 2016;234:27–33.
- [46] Qi Y, Huang Y, Li B, Zeng F, Wu S. Real-Time Monitoring of Endogenous Cysteine Levels In Vivo by near-Infrared Turn-on Fluorescent Probe with Large Stokes Shift. *Anal Chem* 2018;90:1014–20.

- [47] Yang X, Guo Y, Strongin RM. A seminaphthofluorescein-based fluorescent chemodosimeter for the highly selective detection of cysteine. *Org Biomol Chem* 2012;10:2739–41.
- [48] Chen F, Han D, Liu H, Wang S, Li KB, Zhang S. A tri-site fluorescent probe for simultaneous sensing of hydrogen sulfide and glutathione and its bioimaging applications. *Analyst* 2018;143:440–8.
- [49] Nolin T, McMenamin M, Himmelfarb J. Simultaneous determination of total homocysteine, cysteine, cysteinylglycine, and glutathione in human plasma by high-performance liquid chromatography: Application to studies of oxidative stress. *J Chromatogr B* 2007;852:554–61.
- [50] Gao, X, Li X, Li L, Zhou J, Ma H. A simple fluorescent off-on probe for the discrimination of cysteine from glutathione. *Chem Commun* 2015; 51: 9388–90.
- [51] Li Z, He X, Wang Z, Yang R, Shi W, Ma H. *in vivo* imaging and detection of nitroreductase in zebrafish by a new near-infrared fluorescence off-on probe. *Biosen Bioelectron* 2015;63:112–6.

List of Captions

Scheme 1. Chemical structure of NOF1, and the process of detection of Cys *in vitro* and *in vivo*

Scheme 2. Proposed mechanism for sensing of NOF1 for Cys

Figure 1. (a) UV-vis absorption and (b) fluorescence spectral changes of NOF1 (10 μM) upon addition of different concentrations Cys (from 0 to 1.4 eq.) in PBS (5 mM, pH=7.4) with 50 % DMSO (v/v) at 37 °C for 10 min. Inset: Color changes in NOF1 upon addition of Cys (10 μM), $\lambda_{\text{ex}}=670$ nm

Figure 2. (a) Time course of the fluorescence response at 741 nm. Inset: color changes in NOF1 upon addition of Cys, Hcy, and GSH (2.0 eq.). (b) Emission spectral changes of NOF1 in the absence (blank) and presence of Cys, Hcy, and GSH (2.0 eq.) in PBS (5 mM, pH=7.4) with 50% DMSO (v/v). [NOF1] = 10 μM , $\lambda_{\text{ex}} = 670$ nm, 37 °C

Figure 3. (a) Absorption spectra of probe NOF1 (10 μM) treated with various analytes (10.0 eq.). (b) Color change of probe NOF1 (10 μM) treated with 10.0 eq. of various analytes. All experiments were performed in PBS (5 mM, pH=7.4) with 50% DMSO (v/v) at 37 °C for 10 min

Figure 4. (a) Absorption and (b) fluorescence spectra of NOF1 (10 μM) and the product of NOF1 (10 μM) reacted with Cys (1.0 eq.) and NOF1-Cys (10 μM) in PBS (5 mM, pH=7.4) with 50 % DMSO (v/v), $\lambda_{\text{ex}}= 670$ nm

Figure 5. HR-MS spectrum of NOF1 (left side) and NOF1+Cys (right side)

Figure 6. Confocal luminescence images of living HeLa cells. (a) HeLa cells incubated with NOF1 (5 μM) for 30 min at 37 °C. (b) HeLa cells were pretreated with NEM (100 μM) for 120 min and then further incubated with NOF1 (5 μM) for 30 min at 37 °C. (c) HeLa cells were pretreated with Cys (100 μM) for 120 min and then further incubated with NOF1 (5 μM) for 30 min at 37 °C. Emission was collected by an NIR channel at 655–755 nm, under excitation with 635 nm laser. Scale bar = 30 μm

Figure 7. *In vivo* images of zebrafish treated with NOF1. (a) 4-day-old zebrafish was incubated with 10 μM NOF1 for 30 min. (b) 4-day-old zebrafish was pre-incubated with 200 μM NEM for 30 min and then incubated with 10 μM NOF1 for 30 min

Figure 8. Fluorescence imaging of endogenous Cys in living mice injected with NOF1 (25 μM , 50 μL) in saline at 5 min (a) and 30 min (b) after subcutaneous injection. Emission was collected by an NIR channel at 660–780 nm, under excitation with 635 nm laser.

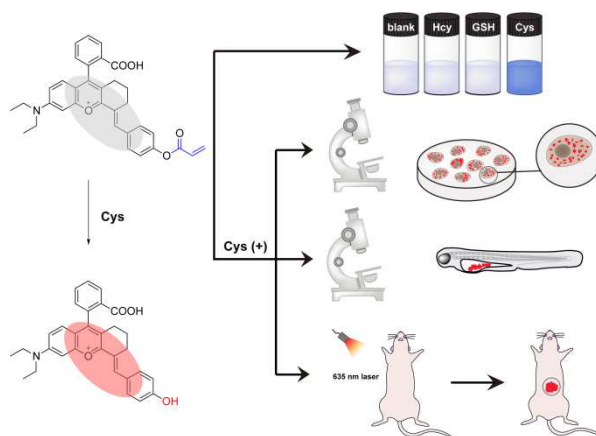
Table 1. Determination of Cys in human plasmas with probe NOF1

Table 1 Determination of Cys in human plasma with probe NOF1

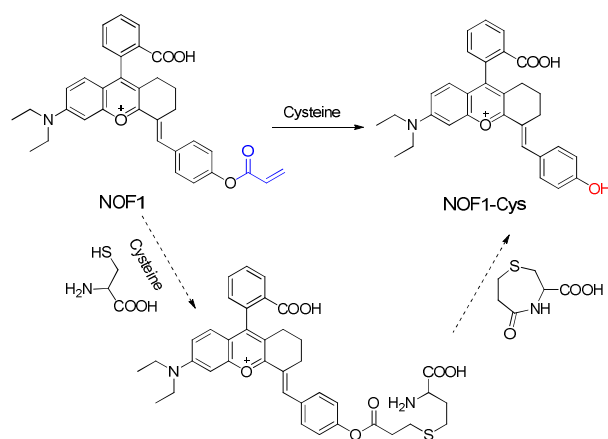
Analyte in plasmas	Added (μM)	found ^a (μM)	Recovery ^a (%)
Cys	0	$1.04^b \pm 0.05$	—
	2	3.11 ± 0.03	102 ± 2.0
	4	5.05 ± 0.03	98 ± 1.1
	6	7.12 ± 0.02	101 ± 3.0

^a Mean of three determinations \pm standard deviation

^b Mean of three determinations after human plasma diluted 160-fold



Scheme 1. Chemical structure of NOF1, and the process of detection of Cys *in vitro* and *in vivo*



Scheme 2. Proposed mechanism for sensing of NOF1 for Cys

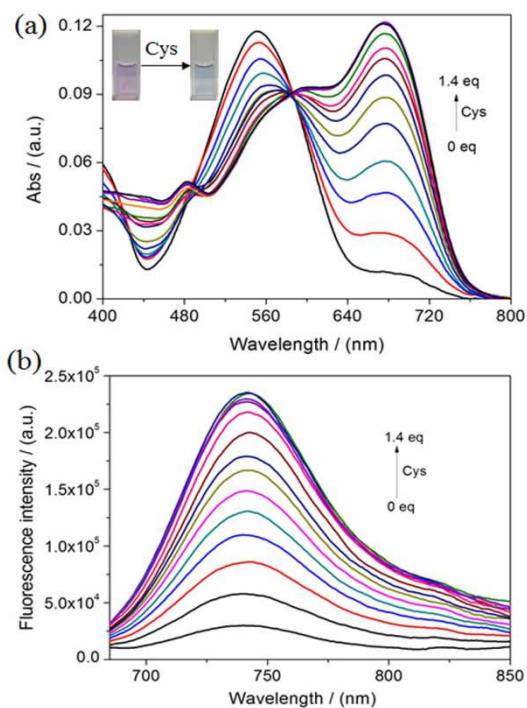


Figure 1. (a) UV-vis absorption and (b) fluorescence spectral changes of NOF1 (10 μM) upon addition of different concentrations Cys (from 0 to 1.4 eq.) in PBS (5 mM, pH=7.4) with 50 % DMSO (v/v) at 37 $^{\circ}\text{C}$ for 10 min. Inset: Color changes in NOF1 upon addition of Cys (10 μM), $\lambda_{\text{ex}}=670$ nm

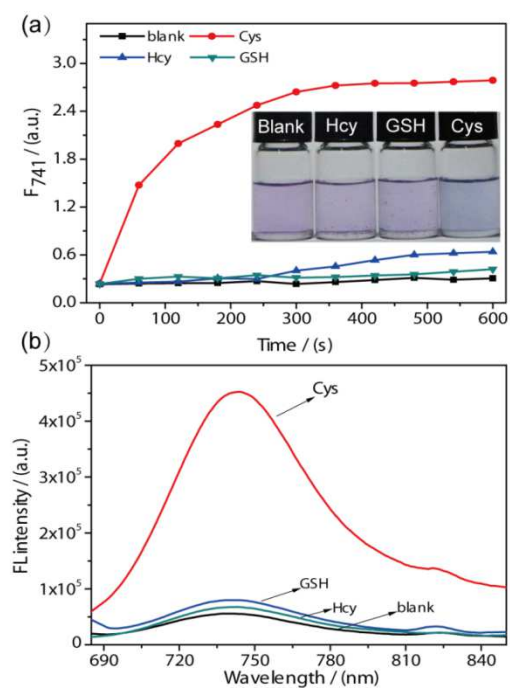


Figure 2. (a) Time course of the fluorescence response at 741 nm. Inset: color changes in NOF1 upon addition of Cys, Hcy, and GSH (2.0 eq.). (b) Emission spectral changes of NOF1 in the absence (blank) and presence of Cys, Hcy, and GSH (2.0 eq.) in PBS (5 mM, pH=7.4) with 50% DMSO (v/v). [NOF1] = 10 μ M, λ_{ex} = 670 nm, 37 $^{\circ}$ C

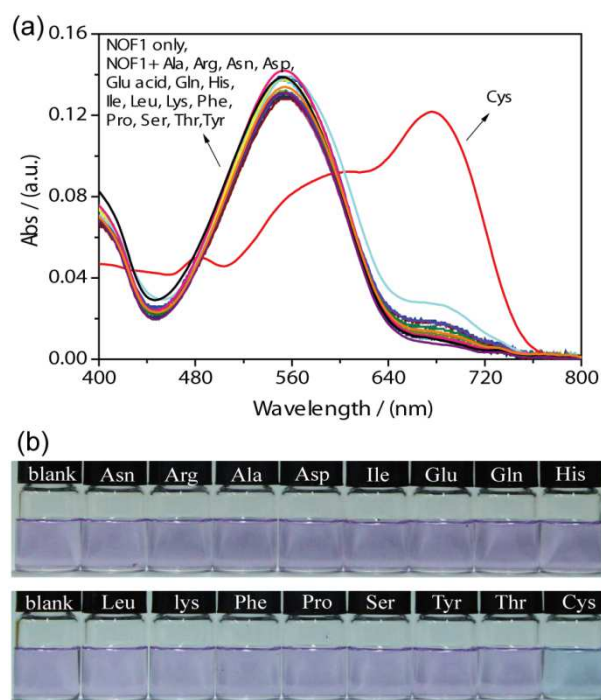


Figure 3. (a) Absorption spectra of probe NOF1 (10 μ M) treated with various analytes (10.0 eq.). (b) Color change of probe NOF1 (10 μ M) treated with 10.0 eq. of various analytes. All experiments were performed in PBS (5 mM, pH=7.4) with 50% DMSO (v/v) at 37 $^{\circ}$ C for 10 min

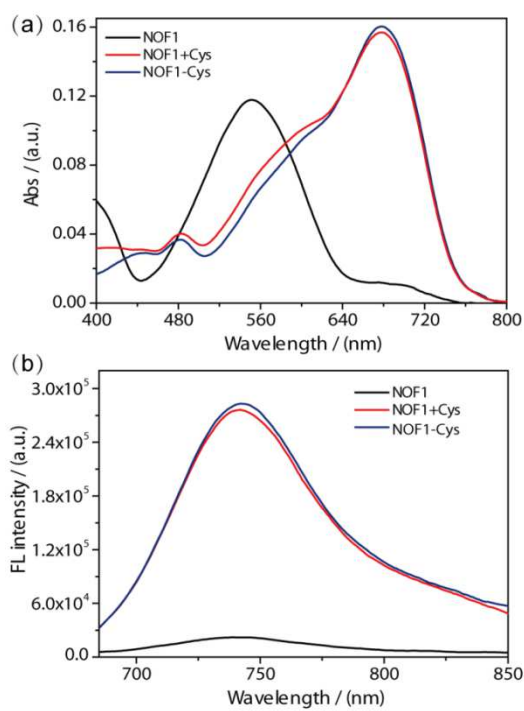


Figure 4. (a) Absorption and (b) fluorescence spectra of NOF1 (10 μM) and the product of NOF1 (10 μM) reacted with Cys (1.0 eq.) and NOF1-Cys (10 μM) in PBS (5 mM, pH=7.4) with 50 % DMSO (v/v), $\lambda_{\text{ex}}=670$ nm

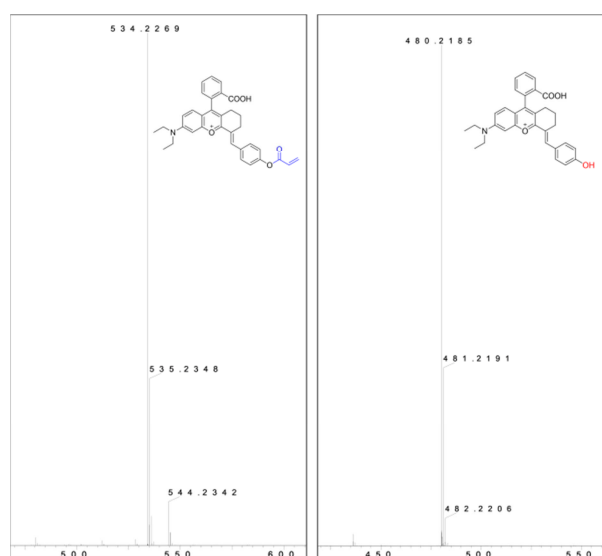


Figure 5. HR-MS spectrum of NOF1 (left side) and NOF1+Cys (right side)

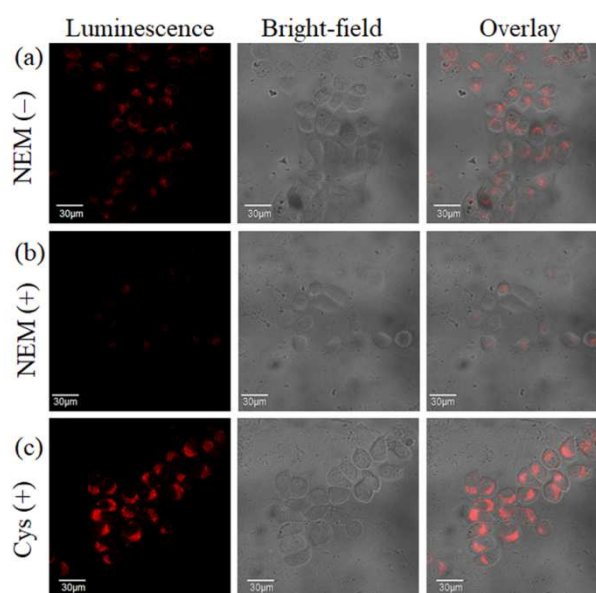


Figure 6. Confocal luminescence images of living HeLa cells. (a) HeLa cells incubated with NOF1 (5 μ M) for 30 min at 37 °C. (b) HeLa cells were pretreated with NEM (100 μ M) for 120 min and then further incubated with NOF1 (5 μ M) for 30 min at 37 °C. (c) HeLa cells were pretreated with Cys (100 μ M) for 120 min and then further incubated with NOF1 (5 μ M) for 30 min at 37 °C. Emission was collected by an NIR channel at 655–755 nm, under excitation with 635 nm laser. Scale bar = 30 μ m

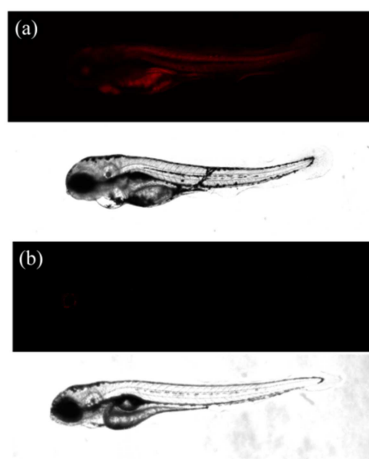


Figure 7. *In vivo* images of zebrafish treated with NOF1. (a) 4-day-old zebrafish was incubated with 10 μ M NOF1 for 30 min. (b) 4-day-old zebrafish was pre-incubated with 200 μ M NEM for 30 min and then incubated with 10 μ M NOF1 for 30 min

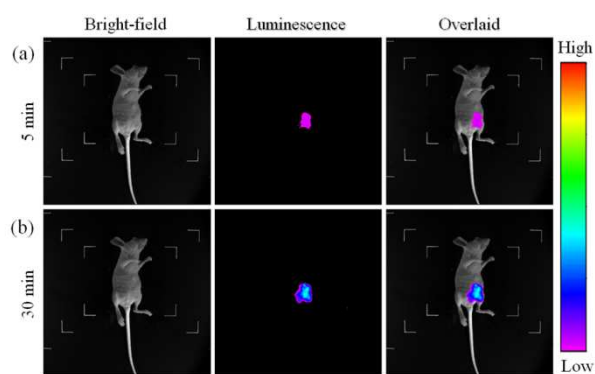


Figure 8. Fluorescence imaging of endogenous Cys in living mice injected with NOF1 (25 μ M, 50 μ L) in saline at 5 min (a) and 30 min (b) after subcutaneous injection. Emission was collected by an NIR channel at 660–780 nm, under excitation with 635 nm laser.

Highlights

- ▶ A simple strategy to synthesize a novel near-infrared xanthene fluorescence sensor for Cys detection.
- ▶ Powerful selectivity and sensitivity for Cys was achieved to differentiate similar bio-thiols (Hcy and GSH).
- ▶ Practical applicability of our sensor for accurately quantifying Cys levels in the human plasma with a good recovery rate.
- ▶ The sensor as a versatile probe was introduced to detect or image Cys in living cells, zebrafish, and mice.